Prepri
UCRL-JC-1373

High-resolution gamma-ray spectrometers using bulk absorbers coupled to Mo/Cu multilayer superconducting transition-edge sensors

D. T. Chow, A. Loshak, M. L. van den Berg, M. Frank, T. W. Barbee Jr., and S. E. Labov

This article was submitted to
Society of Photo-Optical Instrumentation Engineers
45th Annual Meeting
San Diego, CA
July 30 – August 4, 2000

U.S. Department of Energy
Lawrence Livermore National Laboratory

July 4, 2000

Approved for public release; further dissemination unlimited

DISCLAIMER

This document was prepared as an account of work sponsored by an agency of the United States Government. Neither the United States Government nor the University of California nor any of their employees, makes any warranty, express or implied, or assumes any legal liability or responsibility for the accuracy, completeness, or usefulness of any information, apparatus, product, or process disclosed, or represents that its use would not infringe privately owned rights. Reference herein to any specific commercial product, process, or service by trade name, trademark, manufacturer, or otherwise, does not necessarily constitute or imply its endorsement, recommendation, or favoring by the United States Government or the University of California. The views and opinions of authors expressed herein do not necessarily state or reflect those of the United States Government or the University of California, and shall not be used for advertising or product endorsement purposes.

This is a preprint of a paper intended for publication in a journal or proceedings. Since changes may be made before publication, this preprint is made available with the understanding that it will not be cited or reproduced without the permission of the author.

This report has been reproduced
directly from the best available copy.

Available to DOE and DOE contractors from the
Office of Scientific and Technical Information
P.O. Box 62, Oak Ridge, TN 37831
Prices available from (423) 576-8401
http://apollo.osti.gov/bridge/

Available to the public from the
National Technical Information Service
U.S. Department of Commerce
5285 Port Royal Rd.,
Springfield, VA 22161
http://www.ntis.gov/

OR

Lawrence Livermore National Laboratory
Technical Information Department's Digital Library
http://www.llnl.gov/tid/Library.html

High-resolution gamma-ray spectrometers using bulk absorbers coupled to Mo/Cu multilayer superconducting transition-edge sensors

D.T. Chow[a,b], A. Loshak[b], M.L. van den Berg[b], M. Frank[b], T.W. Barbee Jr.[b], S.E. Labov[b]

[a]Department of Applied Science, University of California, Davis
[b]Lawrence Livermore National Laboratory, Livermore, CA, 94550

ABSTRACT

In x-ray and gamma-ray spectroscopy, it is desirable to have detectors with high energy resolution and high absorption efficiency. At LLNL, we have developed superconducting tunnel junction-based single photon x-ray detectors with thin film absorbers that have achieved these goals for photon energies up to 1 keV. However, for energies above 1 keV, the absorption efficiency of these thin-film detectors decreases drastically. We are developing the use of high-purity superconducting bulk materials as microcalorimeter absorbers for high-energy x-rays and gamma rays. The increase in absorber temperature due to incident photons is sensed by a superconducting transition-edge sensor (TES) composed of a Mo/Cu multilayer thin film. Films of Mo and Cu are mutually insoluble and therefore very stable and can be annealed. The multilayer structure allows scaling in thickness to optimize heat capacity and normal state resistance. We measured an energy resolution of 70 eV for 60 keV incident gamma-rays with a $1 \times 1 \times 0.25$ mm^3 Sn absorber. We present x-ray and gamma-ray results from this detector design with a Sn absorber. We also propose the use of an active negative feedback voltage bias to improve the performance of our detector and show preliminary results.

Keywords: Microcalorimeter, cryogenic detector, gamma-ray spectroscopy

1. INTRODUCTION

At the Lawrence Livermore National Laboratory, we are interested in the development of high energy resolution, high efficiency gamma-ray spectrometers for nuclear non-proliferation and arms control programs. Nuclear materials intended for different purposes such as power plants and weapons have different isotopic abundances. High energy resolution gamma-ray spectrometers can be used to determine the isotopic composition of nuclear materials to high accuracy. These spectrometers may also be used to analyze contamination by radioactive materials. Trace elements may be identified by their unique gamma-ray spectrum.

Commercially available semiconductor ionization detectors operate by excitation of electron-hole pairs created by incident photons. The optimal resolution of these detectors is limited by the cascade statistics of the electron-hole pairs. For germanium ionization detectors, the best possible resolution for a 60 keV photon is 300 eV full width at half maximum (FWHM)[1]. Commercially available germanium detectors have typical energy resolutions greater than 500 eV FWHM for 60 keV gamma-rays. Furthermore, the theoretical resolution of semiconducting detectors scale with energy such that at higher energies, the detector will have broader linewidths than at lower energies.

Superconducting materials offer many improvements for radiation detectors. Superconductors have much smaller energy gaps than semiconductors, resulting in a statistical improvement over semiconductor detectors. Our research group has had success in the development of superconducting tunnel junctions (STJ) as detectors for low energy x-rays[2,3]. We want to expand the detection range to higher energy x-rays and gamma-rays. Our STJs are thin film devices and have very poor absorption efficiency for more energetic photons. Therefore, we are developing superconducting microcalorimeters using bulk materials as an absorber.

In a low temperature microcalorimeter, the energy resolution is primarily limited by thermal phonon fluctuations. The phonon noise resolution is $\Delta E \approx 2.35\sqrt{kT^2C}$, where k is Boltzman's constant, T is operating temperature, and C is the heat capacity of the device[4]. At low temperatures, superconductors have very small heat capacities, making them ideal materials for a microcalorimeter. In our detector design, the phonon noise is ~20 eV at the operating temperature of 0.1 K. Furthermore, the linewidth is independent of incident photon energy and can provide high resolution over a large energy range.

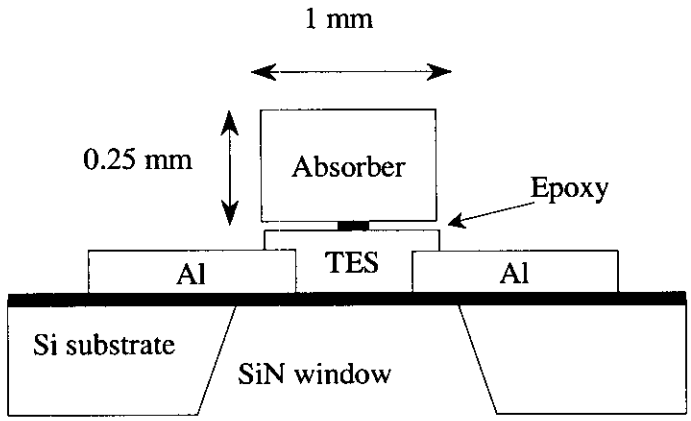

Figure 1: Schematic cross section of gamma-ray microcalorimeter showing the bulk absorber, TES, epoxy, and Al electrical leads fabricated on a SiN membrane window.

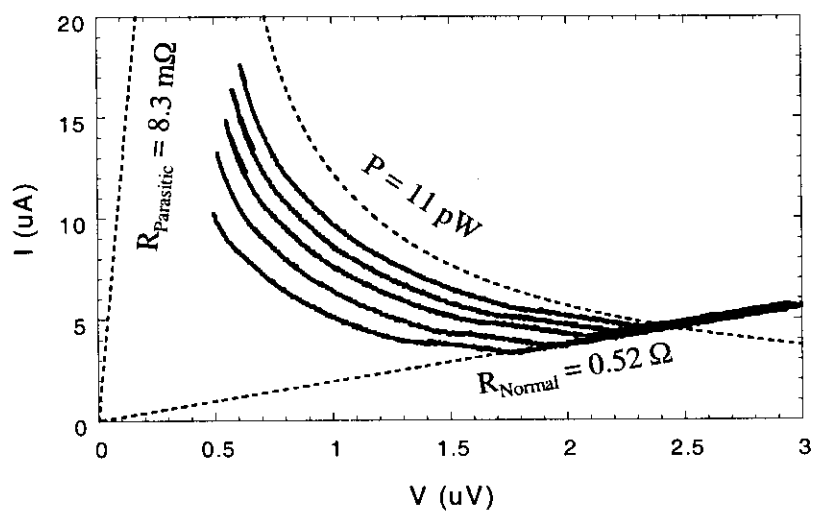

Figure 2: IV characteristics of the detector at different T_{bath}. Lines further from the origin are taken at lower T_{bath}. Dashed radial lines indicate the normal and parasitic resistances. Dashed hyperbolic line represents a constant power contour.

2. DETECTOR DESIGN

The basic elements of a microcalorimeter consist of an absorber, a sensitive thermometer, and a weak thermal link to dissipate energy (figure 1). We have chosen to use high-purity Sn as our absorbing material. Sn has been demonstrated to be a good absorber[5,6,7]. The dimensions of our Sn absorber are $1 \times 1 \times 0.25$ mm^3. The absorptions efficiency is over 70% for 60 keV gamma-rays. The heat capacity of the superconducting Sn absorber $C_{Absorber}$ = 33 keV/mK at the operating temperature T_{op} = 0.1 K.

The bulk absorber is coupled to the thermometer by means of a small (~0.5 μg) amount of Stycast 2850FT epoxy. The Stycast is approximately 100 μm in diameter and 25 μm thick. Stycast is a standard material in cryogenics whose properties are well documented[8]. The heat capacity of the epoxy $C_{Stycast}$ = 30 keV/mK at T_{op} = 0.1 K.

Our thermometer is a superconducting transition edge sensor (TES). A TES is a superconducting film with a very narrow transition between zero resistance and normal resistance such that small changes in temperature cause a large change in resistance. Our TES is a multilayer superlattice of alternating layers of Mo and Cu. These two materials are mutually immiscible, allowing the fabrication of a stable thin film which can also be annealed. Mo is a superconductor at low temperatures, while Cu remains a normal metal. The transition temperature T_c is dictated by the proximity effect and can be tuned by varying the Mo/Cu ratio. The multilayer structure allows the Mo/Cu film to be scaled in thickness without changing T_c. Changing the thickness permits adjustments in normal resistance R_n and heat capacity. The TES has a heat capacity C_{TES} = 5 keV/mK at T_{op} = 0.1 K. The total thickness of the Mo/Cu multilayer is 200 nm.

The absorber and TES are weakly thermally coupled to a cold bath to dissipate the energy from absorbed photons. The weak link is established by fabricating the TES on a 0.5 μm thick silicon nitride (SiN) membrane. In our detector design, we measured the thermal conductivity of SiN G_{SiN} = 0.28 nW/K at the bath temperature T_{bath} = 70 mK. This value is comparable with the theoretical thermal conductivity of 0.32 nW/K for specular phonon scattering[9]. The TES also has superconducting Al leads for electrical contact with negligible thermal conductivity. The TES and the absorber are strongly thermally coupled with $G_{Absorber\text{-}TES}$ ~ 5 nW/K.

3. EXPERIMENTAL SETUP

The detector was tested in an adiabatic demagnetization refrigerator (ADR) capable of reaching a base temperature of 60 mK. The detector output was measured using a voltage-biased circuit with a SQUID-based current amplifier. The voltage bias is provided by a 10 mΩ shunt resistor in parallel with the TES. The voltage bias also allows negative thermal feedback to stabilize the TES on the superconducting transition[10]. The SQUID is a Hypres model #30 single-stage 208 series array with typical noise less than 10 pA/Hz$^{1/2}$.

Operation of the detector is as follows. The detector is voltage biased on the superconducting transition. Incident gamma rays are absorbed in the Sn absorber. Thermal phonons quickly spread from the absorber into the TES, causing a small increase in temperature. The small increase in temperature causes a large increase in the resistance of the TES, which decreases the current flowing through the TES. The absorbed energy slowly flows out into the cold bath via the SiN membrane, thereby restoring the detector to thermal equilibrium. The resulting signal from absorption of a single photon is a current pulse with a fast rise time and a slower decay. Typical values are: bias voltage V_{bias} ~ 1 μV, operating temperature T_{op} ~ 0.1 K, bath temperature T_{bath} ~ 70 mK, operating resistance of TES R_{op} ~ 100 mΩ, current pulse rise time τ_{rise} ~ 100 μs, current pulse decay time τ_{decay} ~ 1 ms.

4. DEVICE CHARACTERISTICS

In figure 2 we show the current-voltage (IV) characteristics of the detector at different bath temperatures. At high voltage bias, the device assumes its normal resistance of 0.52 Ω. At low voltage bias, the device becomes superconducting and exhibits a supercurrent. Note that because the SQUID circuit is a 2-wire measurement, the device's lead resistance of 8.3 mΩ is also measured. Each IV curve is taken at a constant bath temperature. Due to the voltage bias the device operates at near constant power[11]. Radial lines emanating from the origin are lines of constant resistance. Hyperbolas are lines of constant power. The family of IV curves has effectively two independent parameters: operating resistance of the TES (R_{op}), and operating power of the TES (P_{op}). It has been shown experimentally that operating at high P_{op} and low R_{op} gives large current signals[12].

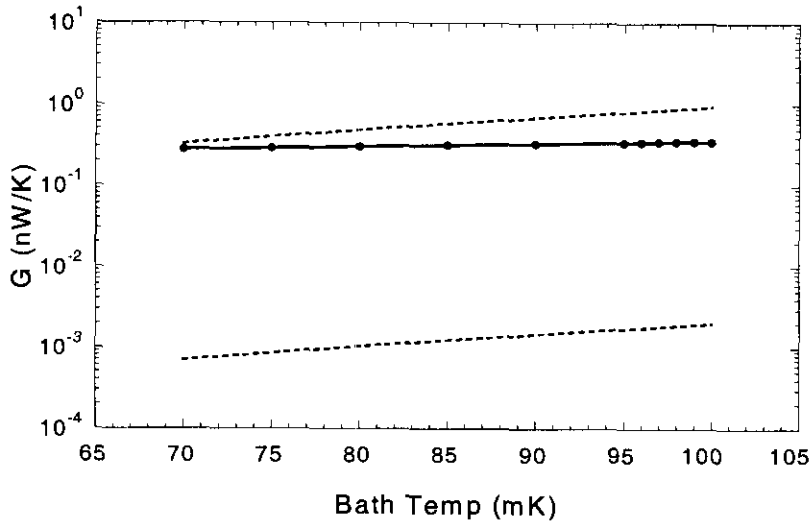

Figure 3: Thermal conductivity of SiN as a function of bath temperature. Upper dashed line is specular limit for phonon scattering. Lower dashed line is dirty limit.

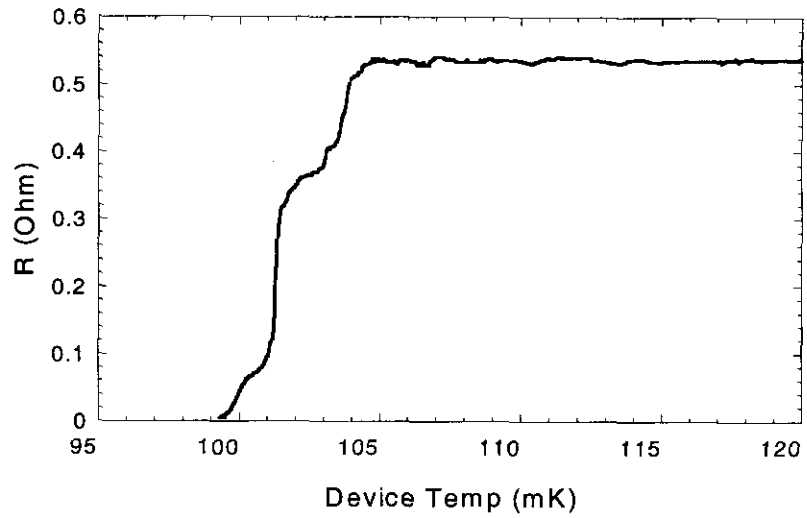

Figure 4: Superconducting transition derived from IV curve. The desirable operating point is on the lower and steeper part of the transition near 0.1 Ω.

From the IV curves we can derive much information. We expect the operating power of the TES to have the following form: $P(T_{bath}) = G_{SiN}(T_{bath}) \times (T_{op}-T_{bath})$, where $G_{SiN}(T_{bath})$ is the thermal conductivity of the SiN membrane as a function of bath temperature. Knowing the operating power at different bath temperatures, we can derive G_{SiN} (figure 3). Comparing with theoretical models for specular scattering and complete diffuse ("dirty") scattering, we see that our SiN membrane is quite "clean". Furthermore, since the dominant phonon wavelengths increase with decreasing temperature, scattering becomes less effective at lower temperatures. We observed G_{SiN} to approach the specular limit with decreasing bath temperature, as expected. At very low temperatures, phonon wavelengths may exceed the dimensions of the SiN membrane and exhibit thermal conductivity better than the specular limit[9].

Once we have determined $G_{SiN}(T_{bath})$, we can calculate the temperature of each point of an IV curve taken at a constant bath temperature. Thus we can map out the superconducting transition by plotting R_{TES} vs. T (figure 4). This method of determining R vs. T is preferred because it allows us to examine the superconducting transition at the actual bias point. Other common means of measuring R vs. T involve applying a current bias and observing the resistance of the TES while changing the bath temperature. This method is often inadequate because it can only be made using a small current bias (<1 μA) and is not representative of actual bias conditions. In microcalorimeter theory, the figure of merit $\alpha = d(\log R)/d(\log T)$ describes the "steepness" of the transition. In this transition, for an operating resistance of $R_{op} = 0.1\ \Omega$ and operating current of $I_{op} = 10$ μA, α is about 600.

5. GAMMA-RAY SPECTRA

Radiation from an ^{241}Am source was measured and a single pulse from one 60 keV photon is shown in figure 5. We measured a pulse height of ~5.5 μA. The pulse rise time is ~170 μs. Pulse decay time is ~0.9 ms. We also note that in the tail of the pulse there is a "kink" which is seen in all pulses taken at this energy. This feature results from non-linearity of the superconducting transition above the operating resistance of 105 mΩ.

In figure 6 we show a spectrum obtained with the ^{241}Am source. In addition to 60 keV photons, we also observed L-lines from the decay product Np. Since the absorber is Sn, there are Sn escape lines in the spectrum. The energetic Np L-lines also excited Cu fluorescence from the detector mount.

With optimal bias and filtering, we achieved an energy resolution of 70 eV FWHM for 60 keV gamma rays. The calculated phonon noise, Johnson noise, and SQUID amplifier noise contributes 22 eV, 5.2 eV, and 3 eV, respectively. The quadrature sum of calculated noise sources is 23 eV. The measured baseline noise is 57 eV. The difference between calculated noise and measured baseline noise is attributed to 60 Hz pick-up. The difference between measured baseline noise and spectrum linewidth is attributed to bias point instability and pile-up events. We are currently improving our measurement system to reduce the effects of pickup and drifts. As described below, we are also working to decrease the pulse length which will move the signal bandwidth away from the 60 Hz noise.

6. ACTIVE FEEDBACK

In the inset of figure 6, we show the detector response as a function of energy. The detector exhibits some deviations from linearity due to non-linearities in the superconducting transition. The microcalorimeter is prone to these imperfections. "Kinks" in the transition may arise from a variety of causes, such as contamination in the TES film, poor photolithography during microfabrication, and stress exerted on the TES film by the epoxy. Gamma-ray spectrometers need to be able to measure over a large range of energy (3 keV to 500 keV). A detector with a highly non-linear response is extremely undesirable.

Another limiting feature of the microcalorimeter is the relatively slow count rate. Because the microcalorimeter depends on complete thermalization of the photon energy, the recovery time of the detector is slow compared to athermal systems such as STJ photon detectors. The pulse length has been shortened significantly by operation in the extreme electrothermal feedback mode[13]. Electrothermal feedback uses the reduction in Ohmic Joule heating (due to a constant voltage bias) during a pulse to speed up recovery of the detector back to its equilibrium state. The natural decay time constant $\tau = C_{total}/G_{SiN}$ of the detector is 40 ms. For this particular operating point, the electrothermally reduced decay time is less than 1 ms. Even so, the count rate is limited to about 50 Hz with negligible pile-up.

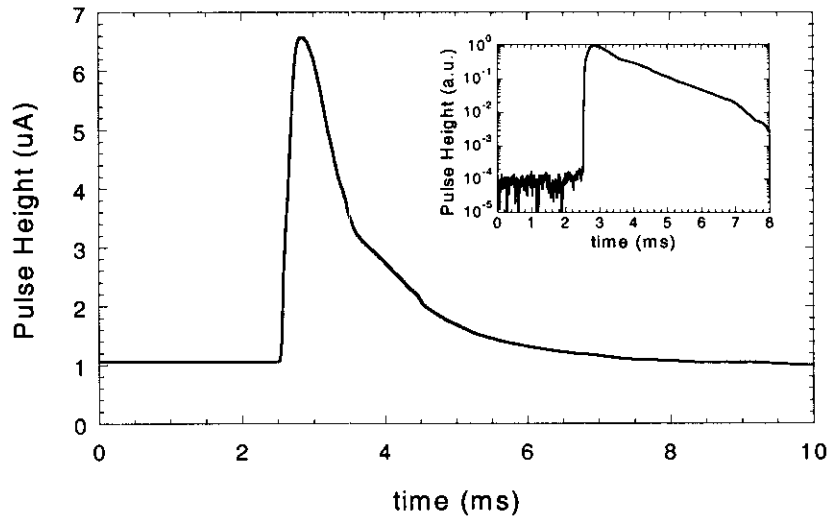

Figure 5: A current pulse from a 60 keV gamma-ray. This is not an averaged pulse, but a single pulse from measuring one photon. Inset shows same pulse normalized on log scale.

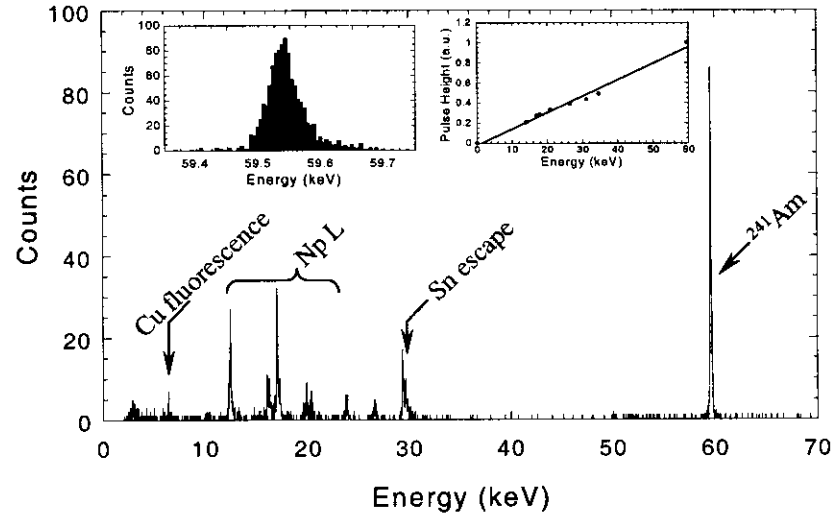

Figure 6: ^{241}Am spectrum showing 60 keV gamma-rays, Sn escape lines, Np L-lines, and Cu fluorescence. Insets shows the 60 keV peak in more detail and detector response. The detector exhibits some deviation from linear response due to non-linearities in the superconducting transition near the operating point.

The pulse length can be further shortened by use of an active negative feedback voltage bias[14]. In this mode of operation, the voltage bias is actively reduced in proportion with the current signal such that the reduction in Joule heating is greater than that of traditional electrothermal feedback, allowing even faster recovery of the detector.

An interesting feature of the active negative feedback voltage bias is that, when operated with the optimal gain settings, the TES will maintain a nearly constant temperature during a pulse. When a photon is absorbed and the thermal energy begins to flow into the TES thermometer, the active negative feedback immediately reduces the bias power of the TES to compensate for the excess heat, effectively maintaining the TES at near constant temperature. For the TES thermometer biased on the transition, a constant operating temperature corresponds to a constant operating resistance. In this "phase locked" mode, a microcalorimeter is impervious to kinks in the transition and will respond linearly with energy. Furthermore, the energy range of the detector will be extended, allowing detection of higher energy gamma-rays without introducing strong non-linearities provided that the equilibrium bias power is sufficiently high.

We have extensively modeled our detector operating with an active negative feedback voltage bias and have begun implementation of this operational mode in our latest detector. We show a schematic of the bias circuit in figure 7. $V_{Bias\,0}$ is the equilibrium bias voltage. During a pulse, TES current decreases and is measured by the SQUID as V_{Signal}. V_{Signal} is fed back, via a summing amplifier, to reduce V_{Bias}. With both the current and voltage of the TES decreasing during a pulse, Joule heating in the TES is reduced greatly.

The active negative feedback bias voltage was implemented in a detector with properties slightly different than the one described above. Results from first measurements of this detection scheme are shown in figure 8 compared with numerical models. All parameters used in the model are calculated from published material properties and known device operating conditions. We see that measured current pulses agree reasonably with the model in both feedback and non-feedback operating modes. For each pulse, we measured both the current and voltage of the TES, which are related by the gain of the summing amplifier. From this, we can calculate the resistance of the TES during the pulse. For this particular bias point, we observed that the change in resistance due to absorption of a gamma-ray photon was reduced by an order of magnitude with active feedback bias, as expected. In our detector design using active negative feedback bias, the shortened pulse decay time is limited by $(C_{Absorber}+C_{Stycast})/G_{Absorber\text{-}TES} \sim 1.9$ ms. We also observed a reduction in pulse length from 2.6 ms to 1.9 ms, as expected. In order to shorten the decay time further, we need to increase the thermal conductivity between the absorber and the TES by increasing the contact area and decreasing the thickness of the epoxy. But at the same time, the total volume of the epoxy should be decreased to reduce the heat capacity. We are currently developing techniques to improve our attachment procedure in a more automated and controlled fashion. The detector used in this measurement responded linearly over the energy range of interest without the aid of the active feedback, so we were unable to demonstrate this aspect of the active feedback bias.

We are confident that when detector geometry and operating conditions are optimized, we will attain a shortened pulse decay time of ~100 μs, which corresponds to a count rate of 500 Hz. Since the total heat capacity of the detector is not limited by the absorber, we can increase the size of the absorber. We will also use higher-Z superconductors as our absorbers to improve absorption efficiency. For gamma-ray spectrometry, we intend to fabricate an array of detectors. For example, a 25-element array of $2 \times 2 \times 0.25$ mm^3 detectors with shortened pulse decay times of ~100 μs will have an effective collection area of 1 cm^2 with a total count rate of >10 kHz. Our gamma-ray spectrometer system will be able to achieve high energy resolution, high count rate, and linear response over a large energy detection range.

7. CONCLUSION

We have developed a superconducting gamma-ray microcalorimeter with a $1 \times 1 \times 0.25$ mm^3 high-purity bulk Sn absorber coupled to a Mo/Cu multilayer TES. We have achieved an energy resolution of 70 eV for 60 keV gamma-rays. The phonon-limited theoretical energy resolution is 23 eV. To further improve the performance of our detector, we proposed the use of an active negative feedback bias for the operation of these detectors to increase count rate, improve the linearity of the detector response, and extend the energy range of the detector. First results of this operational mode has demonstrated proof of principle and feasibility. Other improvements to be implemented include using a larger absorber for more collection area, high-Z absorber for better absorption efficiency, higher bias power for larger energy detection range, better coupling between the absorber and the TES for higher count rate, and arraying. We expect full optimization of the detector system in the near future.

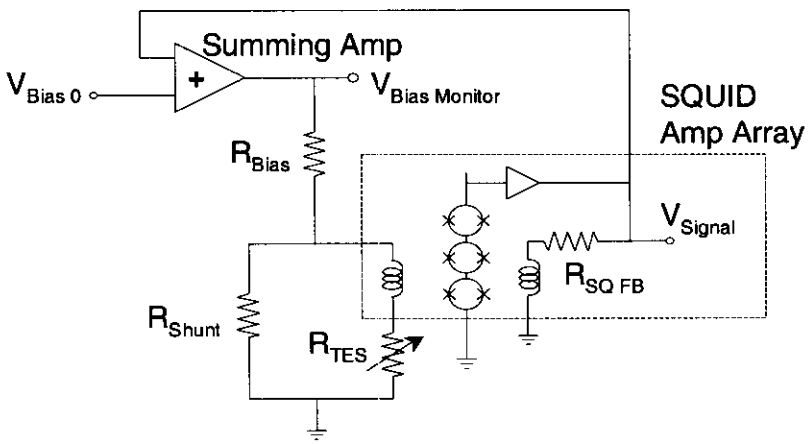

Figure 7: Active feedback voltage bias circuit. The TES is represented by a variable resistor. SQUID components are enclosed within the dashed box. Note that V_{signal} is a negative pulse, so the summing amplifier reduces $V_{Bias\ 0}$. Bias voltage applied during a pulse is monitored at $V_{Bias\ Monitor}$.

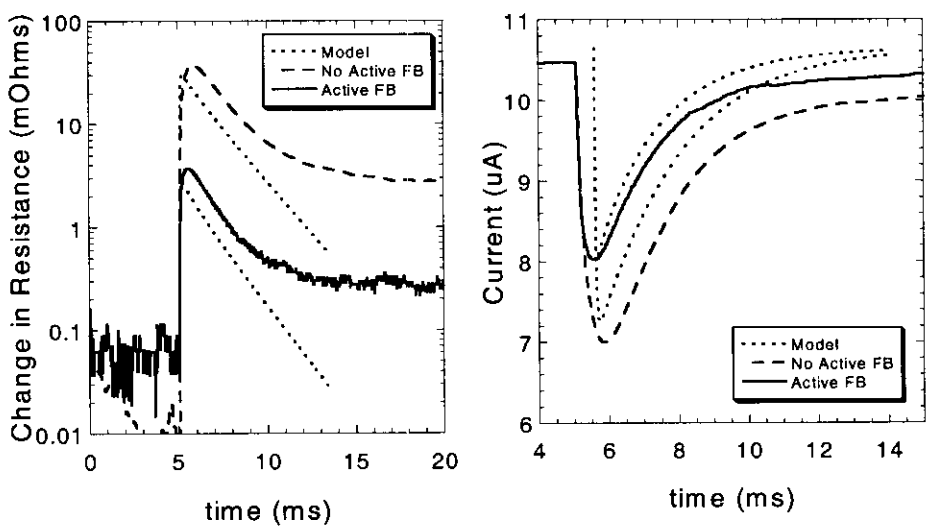

Figure 8: Comparison of signals operating with active feedback (solid lines) and without active feedback (dashed lines). Dotted lines are numerical models of each respective case.

8. ACKNOWLEDGEMENTS

Many thanks to Jan Batteux for excellent experimental and technical support. This work was performed under the auspices of the U.S. Department of Energy by University of California Lawrence Livermore National Laboratory under contract No. W-7405-Eng-48, with support from NASA Constellation-X Technology Development Program under interagency agreement S10256-G and the NASA High Energy Astrophysics Supporting Research and Technology Program under interagency agreement W-19, 121.

9. REFERENCES

[1] Knoll, G.F., "Radiation Detection and Measurement", *John Wiley & Sons, New York*, 1999.

[2] Mears, C.A., Labov, S.E., Frank, M., Lindeman, M., Hiller, L.J., Netel, H., Barfknecht, A.T., "Analysis of pulse shape from a high-resolution superconducting tunnel junction x-ray spectrometer", *Nucl. Instr. Meth. A*, **370**, 53-56, 1996.

[3] Frank, M, Hiller, L.J., le Grand, J.B., Mears, C.A., Labov, S.E., Lindeman, M.L., Netel, H., Chow, D., Barfknecht., A.T., "Energy Resolution and High Count Rate Performance of Superconducting Tunnel Junction X-Ray Spectrometers", *Rev. Sci. Inst.*, **69** (1), 25-31, 1998.

[4] Moseley, S.H., Mather, J.C., McCammon, D., "Thermal Detectors as X-Ray Spectrometers", *J. Appl. Phys.*, **56** (5), 1257-1262, 1984.

[5] Silver, E., LeGros, M., Austin, G., Madden, N., Beeman, J., Haller, E., "First Use of NTD Germanium-Based Microcalorimeters for High-Resolution Broadband X-Ray Microanalysis", *X-Ray Spectrom.*, **25**, 265-268, 1997.

[6] Alessandrello, A., Beeman, J.W., Brofferio, C., Cremonesi, O., Fiorini, E., Giuliani, A., Haller, E.E., Monfardini, A., Nucciotti, A., Pavan, M., Pessina, G., Previtali, E., Zanotti, L., "High Energy Resolution Bolometers for Nuclear Physics and X-Ray Spectroscopy", *Phys. Rev. Lett.*, **82** (3), 513-515, 1999.

[7] Egelhof, P., Beyer, H.F., McCammon, D., Feilitzsch, F.v., et al. "Low-temperature X-ray detectors for precise Lamb shift measurements on hydrogen-like heavy ions", *Nucl. Instr. Meth. A*, **444**, 488-491, 2000.

[8] Swenson, C.A., "Linear thermal expansivity (1.5-300 K) and heat capacity (1.2-90 K) of Stycast 2850FT", *Rev. Sci. Instrum.*, **68**, 1312-1315, 1997.

[9] Holmes, W., Gildemeister, J.M., Richards, P.L., "Measurement of thermal transport in low stress silicon nitride films", *Appl. Phys. Lett.*, **72**, 2250-2252, 1998.

[10] Irwin, K.D., Hilton, G.C., Wollman, D.A., Martinis, J.M., "X-ray detection using a superconducting transition-edge sensor microcalorimeter with electrothermal feedback", *Appl. Phys. Lett.*, **69**, 1945-1947, 1996.

[11] Irwin, K.D., "Phonon-Mediated Particle Detection Using Superconducting Tungsten Transition-Edge Sensors", *Ph.D. Thesis, Stanford Univ.*, 1995.

[12] Chow, D.T., Lindeman, M.A., Cunningham, M.F., Frank, M., Barbee Jr., T.W., Labov, S.E., "Gamma-ray spectrometers using a bulk Sn absorber coupled to a Mo/Cu multilayer superconducting transition edge sensor", *Nucl. Instr. Meth. A*, **444**, 196-200, 2000.

[13] Lindeman, M.A., "Microcalorimetry and the Transition-Edge Sensor", *Ph.D. Thesis, Univ. of Calif., Davis*, 2000.

[14] Nam, S.W., Cabrera, B., Colling, P., Clarke, R.M., Figueroa-Feliciano, E., Miller, A.J., Romani, R.W., "A new biasing technique for transition edge sensors with electrothermal feedback", *IEEE Trans. on Appl. Supercond.*, **9**, 4209-4212, 1999.